

# Phthalocyanine-loaded graphene nanoplatform for imaging-guided combinatorial phototherapy

Olena Taratula<sup>1</sup>  
Mehulkumar Patel<sup>2</sup>  
Canan Schumann<sup>1</sup>  
Michael A Naleway<sup>1</sup>  
Addison J Pang<sup>1</sup>  
Huixin He<sup>2</sup>  
Oleh Taratula<sup>1</sup>

<sup>1</sup>Department of Pharmaceutical Sciences, College of Pharmacy, Oregon State University, Portland, OR, USA; <sup>2</sup>Department of Chemistry, Rutgers University-Newark, Newark, NJ, USA

**Abstract:** We report a novel cancer-targeted nanomedicine platform for imaging and prospect for future treatment of unresected ovarian cancer tumors by intraoperative multimodal phototherapy. To develop the required theranostic system, novel low-oxygen graphene nanosheets were chemically modified with polypropylenimine dendrimers loaded with phthalocyanine (Pc) as a photosensitizer. Such a molecular design prevents fluorescence quenching of the Pc by graphene nanosheets, providing the possibility of fluorescence imaging. Furthermore, the developed nanoplatform was conjugated with poly(ethylene glycol), to improve biocompatibility, and with luteinizing hormone-releasing hormone (LHRH) peptide, for tumor-targeted delivery. Notably, a low-power near-infrared (NIR) irradiation of single wavelength was used for both heat generation by the graphene nanosheets (photothermal therapy [PTT]) and for reactive oxygen species (ROS)-production by Pc (photodynamic therapy [PDT]). The combinatorial phototherapy resulted in an enhanced destruction of ovarian cancer cells, with a killing efficacy of 90%–95% at low Pc and low-oxygen graphene dosages, presumably conferring cytotoxicity to the synergistic effects of generated ROS and mild hyperthermia. An animal study confirmed that Pc loaded into the nanoplatform can be employed as a NIR fluorescence agent for imaging-guided drug delivery. Hence, the newly developed Pc-graphene nanoplatform has the significant potential as an effective NIR theranostic probe for imaging and combinatorial phototherapy.

**Keywords:** graphene nanosheets, phthalocyanine, photothermal therapy, photodynamic therapy, theranostic

## Introduction

The high mortality rate among patients with metastatic ovarian cancer is attributed to the fact that only surgical removal of most of its abdominal metastases may reduce cancer recurrence and enhance the effect of postoperative chemotherapy.<sup>1,2</sup> Unfortunately, even with the best microsurgical techniques, resection leaves behind residual microscopic tumors, which eventually lead to cancer relapse.<sup>3</sup> Furthermore, the effect of postoperative chemotherapy is significantly compromised by the resistance of ovarian cancer cells to chemotherapeutic agents and the serious side effects that nontargeted chemotherapeutic agents have on healthy organs.<sup>4</sup> To meet the current medical needs, our goal herein was to develop a novel theranostic nanomedicine platform that enables imaging and maximal treatment of unresected and chemoresistant ovarian cancer cells, using an intraoperative multimodal phototherapy. A synergistic effect of combined noninvasive photodynamic (PDT) and photothermal (PTT) therapy is expected to improve the therapeutic efficiency, overcome multidrug resistance, and decrease the dosage-limiting toxicity of current chemotherapy drugs.<sup>5,6</sup>

PDT is a noninvasive clinical approach for cancer that involves use of a nontoxic photosensitizer, which, after illumination with a specific light, causes the formation of

Correspondence: Oleh Taratula  
Department of Pharmaceutical Sciences,  
College of Pharmacy, Oregon State  
University, 2730 SW Moody Avenue,  
Office CLSB 4N038, Portland,  
OR 97201, USA  
Tel +1 503 346 4704  
Email [oleh.taratula@oregonstate.edu](mailto:oleh.taratula@oregonstate.edu)

cytotoxic reactive oxygen species (ROS) that damage cancer tissue.<sup>7</sup> In addition, when the photosensitizer, upon excitation, is able to produce fluorescence emission, it can act as both a therapeutic and imaging agent. Unlike photosensitizers, PTT agents absorb the light, which is then transformed into heat and transferred to the intracellular environment, generating localized hyperthermia.<sup>8–11</sup> The combination of both PDT and PTT, which are based on different anticancer mechanisms, into a single therapeutic modality offers a highly proficient method to treat ovarian cancer tumors. To avoid multiple administrations of different therapeutic agents and improve patient compliance, it is highly desirable to have a single nanomedicine platform that possesses both the PDT and PTT therapeutic functions.

One of the key challenges in the clinical application of both PDT and PTT is that the visible light required to activate the appropriate therapeutic agents can only penetrate through several millimeters of tissue.<sup>7</sup> Therefore, ideal PDT and PTT agents would strongly absorb in the near-infrared (NIR) transparency window for biological tissues and effectively transform the absorbed energy into ROS and heat, respectively. Furthermore, fluorescence imaging within the NIR tissue optical window is very attractive, thanks to minimal light scattering and tissue autofluorescence. Thus, by monitoring the fluorescence emission of the photosensitizer in metastatic tumors after systemic administration, phototherapy can be more accurately applied to cancerous tissue while leaving healthy tissue unaffected.

Owing to their strong absorption within the NIR window, the second-generation photosensitizers, including phthalocyanine (Pc), have showed significant potential as theranostic agents.<sup>12,13</sup> However, most of these agents are not cancer-specific, are very hydrophobic, and are not easy to formulate.<sup>14</sup> To overcome these barriers and provide additional PTT capability, several delivery systems, based on gold nanoparticles, gold nanorods, and graphene, have been reported.<sup>15,16</sup> Among them, graphene is a highly promising nanomaterial for the development of PDT–PTT nanomedicine platforms.<sup>17</sup> Owing to its large surface area, low cost, broad NIR absorption, and photothermal heating properties, graphene could be a suitable material to immobilize and deliver Pc, with appropriate excitation wavelength to achieve a synergetic PTT–PDT effect.<sup>18–20</sup> However, since the absorption the reported PTT and PDT agents do not overlap, the majority of previously developed systems based on graphene could not be activated with a single light source.<sup>21–25</sup> The sequential irradiation by two lasers of different wavelengths lengthens

the treatment time and requires exact alignment of the two light beams.

Until now, only one nanomedicine platform based on graphene and naphthalocyanine has been developed for single-light-induced PDT–PTT therapy with imaging capability.<sup>26</sup> A noncovalent method was used to immobilize photosensitizers onto graphene via  $\pi$ – $\pi$  stacking, which caused a significant reduction in the fluorescence and ROS generation as a result of a  $\pi$ – $\pi$  stacking interaction with graphene.<sup>21,22,26,27</sup>

To overcome the aforementioned obstacles, we developed a novel ovarian cancer-targeted nanomedicine platform that preserves fluorescence imaging and ROS-generating capabilities of the photosensitizer immobilized on the graphene surface. In our design, graphene nanosheets were chemically conjugated with polypropylenimine generation 4 (PPIG4) dendrimer loaded with silicon Pc derivative to produce a LOGr-Pc-PPIG4 complex (Figure 1). It is worth noting that in addition to the fluorescence quenching of Pc, as a result of  $\pi$ – $\pi$  stacking with graphene oxide, Zhu et al demonstrated that chemical conjugation of nonprotected Pc to graphene oxide also decreases its fluorescence intensity, due to the electron transfer process from the Pc to the graphene oxide.<sup>28</sup> As a PTT agent, we employed novel LOGr nanosheets, fabricated via simple unique microwave preparation, as reported earlier by our team.<sup>29</sup> In contrast to graphene oxide, which is widely used for biomedical applications, LOGr nanosheets have 40-fold stronger light absorption, low density of oxygen-containing groups (similar to reduced graphene oxide), and larger ordered crystallite graphitic domains, of  $\approx 6.7$  nm.<sup>29</sup> As fabricated LOGr nanosheets are easily dispersed in water and exhibit largely preserved intrinsic properties of graphene, they show strong and nearly wavelength-independent NIR absorption, without the need for a postreduction process.<sup>29</sup>

In this particular study, our design allows use of a single excitation wavelength within the NIR therapeutic window to activate both LOGr, for photothermal heating, and Pc, for production of ROS against ovarian cancer (Figure 1). Finally, LOGr-Pc-PPIG4 was functionalized with poly(ethylene glycol) (PEG) and luteinizing hormone-releasing hormone (LHRH) peptide, to assure biocompatibility and tumor-targeting, respectively.<sup>10,30,31</sup> Moreover, without the need to release therapeutic agents following cellular internalization, the prepared formulation acted as a theranostic agent, producing efficient fluorescence emission, ROS, and heat upon light activation, to identify and destroy ovarian cancer cells. The preparation and characterization of LOGr-Pc-LHRH,

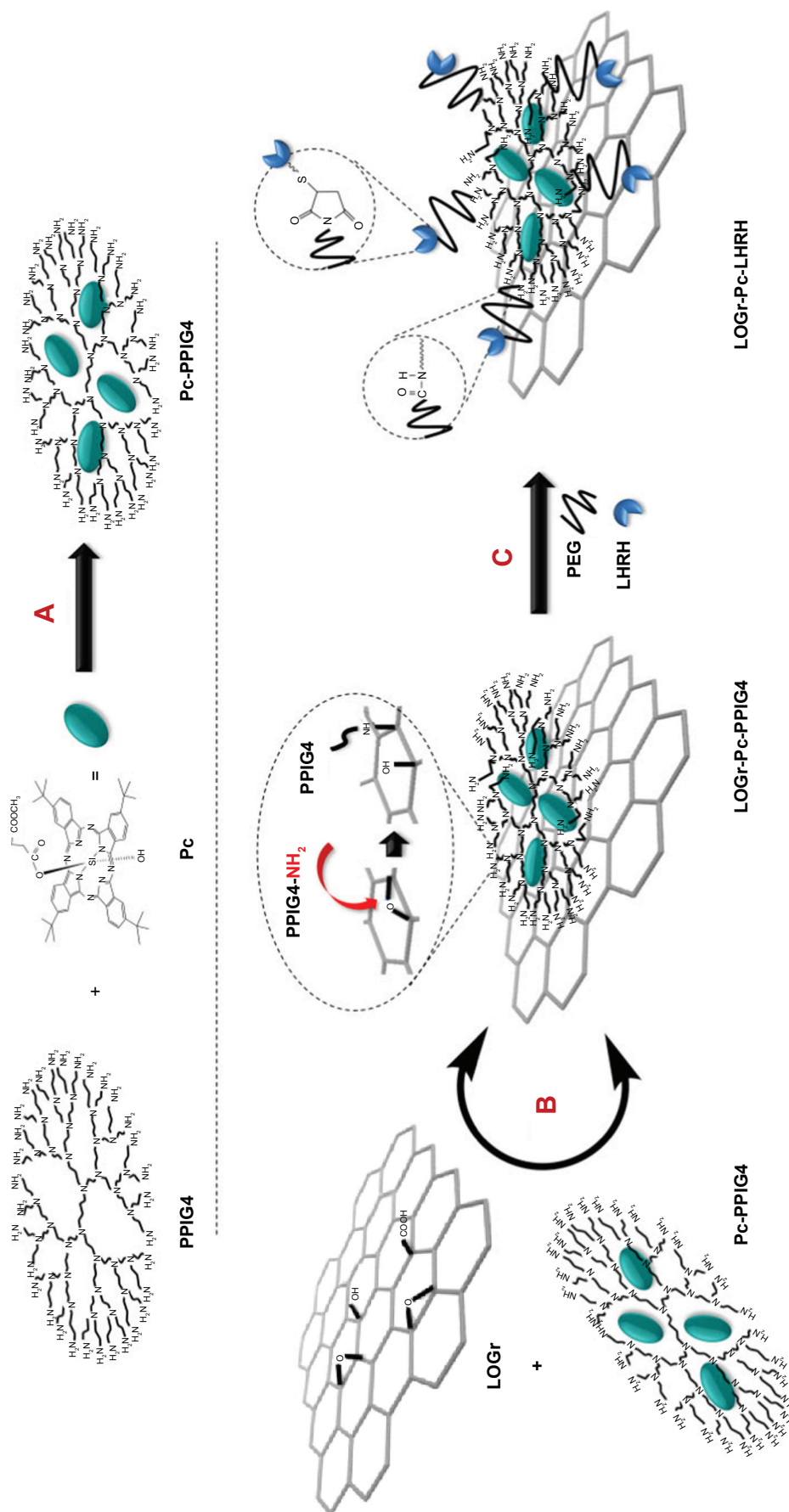


**Figure 1** Schematic illustration of the synthetic procedure for the multifunctional nanoplateform (LOGr-Pc-LHRH).  
**Notes:** (A) Encapsulation of Pc into PPIG4. (B) Conjugation of LOGr nanosheets with the Pc-loaded PPIG4, via a nucleophilic ring-opening reaction between the epoxy groups of LOGr and the amine groups of the PPIG4 dendrimer. (C) Modification of the prepared conjugate (Pc-LOGr) with PEG and LHRH peptide.

**Abbreviations:** LHRH, luteinizing hormone-releasing hormone; LOGr, low-oxygen graphene; Pc, phthalocyanine; PEG, poly(ethylene glycol); PPIG4, polypropyleneimine generation 4.

as well as its *in vitro/in vivo* phototherapeutic and imaging properties, are described below.

## Materials and methods

### Materials

PPIG4 was provided by SyMO-Chem (Eindhoven, the Netherlands). Monosubstituted Pc derivative (PcSi(OH)(mob)) hereinafter referred to as Pc and the PcSi(OH)(mob)-PPIG4-PEG-LHRH complex (Pc-LHRH) were prepared according to the published protocol by our group.<sup>32</sup>  $\alpha$ -Maleimide- $\omega$  (MAL)-N-hydroxysuccinimide (NHS) ester poly(ethylene glycol) (PEG) (MAL-PEG-NHS) (5,000 Da) and LHRH (Lys6–des-Gly10–Pro9-ethylamide [Gln–His–Trp–Ser–Tyr–DLys(DCys)–Leu–Arg–Pro–NH–Et]) peptide were purchased from NOF Corporation (White Plains, NY, USA) and GE Health care (Little Chalfont, UK), respectively. A bicinchoninic acid (BCA) protein assay kit and trinitrobenzene sulfonic acid (TNBSA) were obtained from Thermo Fisher Scientific Inc (Waltham, MA, USA). All other chemicals were of analytical grade.

### General methods

Ultraviolet-visible (UV-Vis) spectra and fluorescence spectra were acquired on a UV-1800 spectrophotometer (Shimadzu Corp, Kyoto, Japan) and Cary Eclipse R3896 fluorescence spectrophotometer (Varian Medical Systems Inc, Palo Alto, CA, USA), respectively. Samples for atomic force microscopy (AFM) were recorded using a multimode scanning probe microscope system (Nanoscope IIIa; Veeco Instruments Ltd, Plainview, NY, USA) (J scanner operated in the “Tapping Mode”), where the sample was drop-casted on a freshly cleaved mica surface and then dried in air or ambient conditions.

### LOGr nanosheets

LOGr nanosheets were prepared by mixing graphite powder with concentrated sulfuric acid (7.0 mL), deionized (DI) water (0.2 mL), and nitric acid (2.8 mL), followed by microwave irradiation (300 W) for 30 seconds, according to the previously published protocol.<sup>29</sup>

### Dendritic graphene nanoplateforms LOGr-PPIG4 and LOGr-Pc-PPIG4

For preparation of the LOGr-PPIG4 conjugate, 1 mL of LOGr aqueous suspension (~0.2 mg/mL) was mixed with 1 mL of PPIG4 dendrimer (10 mg/mL) solution in water. Next, KOH (10 mg) was added into the above mixture, and then the mixture was sonicated for 30 minutes. Finally, the reaction mixture was vigorously stirred at 80°C for 12 hours. Next, size exclusion chromatography (with a Sephadex®

G75 column, 1×18 cm) was employed to purify the modified complexes. The same procedure was used to prepare the LOGr-Pc-PPIG4 conjugate, except that prior to the reaction, the Pc derivative (PcSi(OH)(mob)) was loaded within the PPIG4 dendrimer, with 20% loading, as previously described by our group.<sup>32</sup>

### LOGr-PPIG4-PEG-LHRH (LOGr-LHRH) and LOGr-Pc-PPIG4-PEG-LHRH (LOGr-Pc-LHRH)

For modification of LOGr-PPIG4 with PEG and LHRH, the earlier reported methods were employed.<sup>30,33</sup> Concisely, primary amines of PPIG4 dendrimer were reacted with the NHS groups of the heterobifunctional PEG polymer (MAL-PEG-NHS) (5 kDa) at a molar ratio of 1:16 (primary amines to PEG) in 50 mM (pH 7.4) phosphate-buffered saline (PBS) buffer (Figure 1). After shaking for 1 hour at room temperature, LHRH peptide was added at the molar ratio of 1:1 (MAL-PEG-NHS to LHRH peptide), allowing the reaction, and the mixture was stirred overnight. The peptide was covalently attached to the distal end of the PEG via the reaction between the thiol groups in LHRH and the MAL groups on the PEG (Figure 1). After 12 hours of stirring, size exclusion chromatography (Sephadex G75 column) was used for complexes purification. The decrease in the amount of amino groups on the PPIG4 surface, as well as the amount of amino groups available for PEGylation, was evaluated by a TNBSA assay, as earlier reported.<sup>30</sup> To confirm the LHRH peptide conjugation on the surface of the complex Pc-(OH)(mob)-PPIG4-PEG-LHRH (Pc-LHRH), BCA protein assay was used.<sup>30,33</sup> The same procedure was used to prepare the LOGr-Pc-LHRH conjugate.

UV-Vis absorption was employed to determine the amount of Pc loaded in the dendrimer, with a Q-band at 692 nm in tetrahydrofuran. The concentration of LOGr in the complexes was also determined based on its absorption in water at 808 nm with a mass extinction coefficient of  $-22.7 \text{ mLmg}^{-1}\text{cm}^{-1}$ .<sup>29</sup>

### Zeta potential measurements

Zeta potentials of the prepared complexes were recorded on Malvern ZetaSizer NanoSeries system (Malvern Instruments, Malvern, UK), in PBS buffer (pH 7.4) with a final Pc concentration of 1.0  $\mu\text{g/mL}$  and LOGr concentration of 1.7  $\mu\text{g/mL}$ , respectively, at 25°C.

### Stability

To evaluate the stability of LOGr-Pc-LHRH under physiological conditions, various concentrations, ranging from 1  $\mu\text{g/mL}$  to 50  $\mu\text{g/mL}$ , of LOGr were tested in water, PBS of pH 7.4

alone, and PBS of pH 7.4 containing 10% w/v of fetal bovine serum (FBS), and incubated at 37°C overnight. Then, the samples were centrifuged at 5,000×g and 4°C for 10 minutes. The stability of prepared graphene-based nanoplateform was demonstrated by the absence of precipitate and aggregates.

## Photothermal properties in solution

Aliquots, of 500 µL, of the studied solution were added into a microtube and placed on a heating block at 37°C, 10 minutes prior to irradiation. The solutions of LOGr, LOGr-LHRH, and LOGr-Pc-LHRH (Pc ~15 µg/mL), in Roswell Park Memorial Institute (RPMI) (Corning Inc, Corning, NY, USA) 1640 cell culture medium with 10% FBS, were irradiated at the LOGr concentration of 20 µg/mL, with a continuous wave (CW) laser diode at 690 nm (Intense Ltd, North Brunswick, NJ, USA) (0.95 W/cm<sup>2</sup>) for 20 minutes. The temperature was monitored at designated time intervals with a thermocouple thermometer. As a control, 500 µL of RPMI 1640 medium with 10% fetal bovine serum and Pc-LHRH (Pc ~15 µg/mL) aqueous solution was irradiated for temperature recording at the same laser settings.

## Singlet oxygen (<sup>1</sup>O<sub>2</sub>) measurements

<sup>1</sup>O<sub>2</sub> production was determined by the Singlet Oxygen Sensor Green® (SOSG) assay (Life Technologies, Carlsbad, CA, USA). For the assay, a green fluorescence (excitation/emission maxima ~504/525 nm) of SOSG was recorded in the presence of <sup>1</sup>O<sub>2</sub>. Using a 96-well white plate, 40 µL of the 25 µM stock SOSG solution, 50 µL of D<sub>2</sub>O (EMD Millipore, Billerica, MA, USA), and 10 µL of LOGr-LHRH, Pc-LHRH, or LOGr-Pc-LHRH (Pc ~20 µg/mL, LOGr ~40 µg/mL) solution dissolved in MilliQ water were added into two parallel wells, with working concentrations of 10 µM (SOSG), 2 µg/mL (Pc), and 4 µg/mL (LOGr) in 100 µL per well. Next, one well was irradiated with light (690 nm, 0.3 W/cm<sup>2</sup>, 5 minutes), while the dark control was protected. Instantly, the samples were analyzed on the Cary Eclipse R3896 fluorescence spectrophotometer, using an excitation of 504 nm and emission of 525 nm. All experiments were performed in triplicate.

## Pc-drug release and photostability

The drug release of Pc from LOGr-Pc-LHRH (Pc = 50 µg/mL) was evaluated in the presence of 10 mM reduced glutathione in PBS at pH 7.4 and pH 5.5, as previously reported.<sup>32</sup> The percentage of drug release was calculated according to the formula:

$$\text{Drug release (\%)} = [\text{Pc}]_{\text{R}} / [\text{Pc}]_{\text{T}} \times 100 \quad (1)$$

where [Pc]<sub>R</sub> is the amount of Pc released at collection time, and [Pc]<sub>T</sub> is the total amount of loaded Pc.

To investigate the photostability of Pc in the LOGr-Pc-LHRH nanoplateform, LOGr-Pc-LHRH in PBS of pH 7.4, with the Pc concentration of 50 µg/mL, was irradiated by 690 nm laser diode (0.95 W/cm<sup>2</sup>) for 10 minutes every 12 hours for 96 hours. The concentration of Pc was monitored at fixed time intervals using UV-Vis spectroscopy.

## Hemolytic activity

Hemolysis experiments were carried out according to previously published reports.<sup>32,34</sup> Samples of ethylenediaminetetraacetic acid (EDTA)-stabilized human blood were freshly acquired (Innovative Research Inc., Novi, MI, USA).

## Cell culture

The LHRH receptor-positive A2780/AD multidrug resistant human ovarian carcinoma cell line was purchased from American Type Culture Collection (ATCC), (Manassas, VA, USA). Cells were grown in a humidified atmosphere of 5% CO<sub>2</sub> (v/v) in air at 37°C. Cells were cultured in RPMI 1640 medium with 10% fetal bovine serum and 1.2 mL/100 mL penicillin–streptomycin (Cellgro®).

## Flow cytometry

Cellular internalization of the LHRH-targeted graphene nanoplateform (LOGr-Pc-LHRH) in comparison with the Pc-LHRH was quantified by flow cytometry analysis (BD Accuri™ C6 Flow Cytometer; BD Biosciences, Franklin Lakes, NJ, USA). A2780/AD cells were treated with Pc-LHRH and LOGr-Pc-LHRH for 24 hours at the concentration of 2 µg/mL and 4 µg/mL for Pc and LOGr, respectively. Untreated cells were used as a negative control. After treatment, cells were washed three times with Dulbecco's PBS (DPBS), detached using 0.05% trypsin (Corning Inc) and collected for flow cytometry analysis.

## Cytotoxicity study

The dark (in the absence of light) cellular cytotoxicity was assessed avoiding light, by Calcein AM Cell Viability Assay. Cancer cells were seeded at the density of 10×10<sup>3</sup> cells/well in 96-well microtiter plates and allowed to grow at 37°C for 24 hours. Next, the culture medium was removed, and the cells were treated with 100 µL of medium with different concentrations of Pc (1.10, 2.20, 8.90, 35.7, and 71.0 µg/mL) and LOGr (1.90, 3.90, 15.6, 62.5, and 125.0 µg/mL) for 24 hours. As a control, A2780/AD cells in fresh medium were used. After 24 hours of treatment, the cells were rinsed with DPBS buffer and treated in the

dark with 200  $\mu\text{L}$  of 10  $\mu\text{M}$  calcein AM in DPBS buffer for 1 hour. Fluorescence was recorded using a multiwell plate reader (Synergy HT; Bio Tek Instruments Inc., Winooski, VT, USA) with 485/528 nm excitation/emission filters. Based on these measurements, cellular viability (%) was calculated for each tested sample and expressed as a percentage relative to the untreated control cells. Data were represented as mean values  $\pm$  standard deviation (SD) from minimum of independent measurements. The differences were considered significant at a level of  $P < 0.05$ .

## Combinatorial PDT-PTT treatment

All experimental procedures prior to light treatment were performed under subdued lighting. Irradiation of A2780/AD ovarian cancer cells was realized by placing the cell well on a heating block at 37°C for 10 minutes prior to irradiation. A2780/AD cancer cells were treated in the dark for 18 hours with 100  $\mu\text{L}$  of the LOGr-Pc-LHRH in medium with different concentrations of Pc (1.0, 2.0, and 4.0  $\mu\text{g}/\text{mL}$ ) and LOGr (1.8, 3.5, and 7.0  $\mu\text{g}/\text{mL}$ ). Test samples containing 100  $\mu\text{L}$  of fresh medium were immediately exposed to a 690 nm laser diode at 0.3  $\text{W}/\text{cm}^2$  for 15 minutes (Intense Ltd). Simultaneously, to evaluate the synergetic effect of PDT and PTT, A2780/AD cancer cells were treated with LOGr-LHRH and Pc-LHRH at the same Pc and LOGr concentrations. In addition, different controls were employed: (1) LOGr-LHRH and Pc-LHRH, with no light irradiation (in dark); (2) cells only, treated with light; (3) cells only, in fresh medium; and (4) a medium-only control. After treatment, samples were incubated for a further 24 hours post-light treatment and then evaluated by cell viability calcein AM assay.

To mimic an ovarian cancer tumor, the cell pellets ( $\sim 2$  million cells/vial) treated with LOGr-LHRH, Pc-LHRH, and LOGr-Pc-LHRH (Pc  $\sim 9$   $\mu\text{g}/\text{mL}$ , LOGr  $\sim 15$   $\mu\text{g}/\text{mL}$ ) were irradiated at 690 nm (690 nm, 0.95  $\text{W}/\text{cm}^2$ ) for 10 minutes. After the heating experiment, cells were seeded in a 96-well plate and incubated for 24 hours, at 37°C. Cell viability was determined by calcein AM assay.

The combined effect of the combinatorial treatment was assessed by Valeriote's method.<sup>10</sup> The combined effects were defined as follows: synergistic effect was found when  $(A + B) < (A) \times (B)/100$ ; additive effect was found when  $(A + B) = (A) \times (B)/100$ ; subadditive effect was found when  $(A) \times (B)/100 < (A + B) < (A)$ , if  $(A) < (B)$ ; interference effect was found when  $(A) < (A + B) < (B)$ , if  $(A) < (B)$ ; and antagonistic effect was found when  $(B) < (A + B)$ , if  $(A) < (B)$ , where  $(A)$ ,  $(B)$ , and  $(A + B)$

represent the percentage of cell viability for treatments A (PTT) and B (PDT) and A + B (combinatorial treatment).

## ROS measurements

Intracellular ROS was evaluated using a 2',7'-dichlorodihydrofluorescein diacetate (DCFH-DA) assay.<sup>32,35</sup> Concisely, A2780/AD cells were treated with LOGr-Pc-LHRH at Pc concentration of 2.0  $\mu\text{g}/\text{mL}$  (LOGr 3.5  $\mu\text{g}/\text{mL}$ ) for 24 hours. The next day, the cells were rinsed with DPBS, and 100  $\mu\text{L}$  of 10  $\mu\text{M}$  DCFH-DA was added under dark, 30 minutes before light treatment. The samples were irradiated with a 0.3  $\text{W}/\text{cm}^2$  laser diode light of 690 nm for 5 minutes. LOGr-LHRH and Pc-LHRH of the same concentration were also tested for ROS production. In addition, the cell-only control, LOGr-LHRH, and Pc-LHRH, without light treatment, were used as a dark control. The controls used were cells only and cells only that were irradiated with light, these were considered as 1% and used to demonstrate minimal ROS production. Fluorescence of the DCFH-DA probe was recorded on a plate reader with 485/528 nm excitation/emission filters.

## In vivo imaging

An animal (nude mice) model of human ovarian carcinoma xenografts was developed, according to a previous protocol.<sup>32</sup> Concisely, A2780/AD human ovarian cells ( $5 \times 10^6$  cells) were subcutaneously introduced into the right flank of female athymic mice (total five mice). After 10–12 days, when the tumors reached a size of about 100  $\text{mm}^3$ , the mice were treated with tumor-targeted LOGr-Pc-LHRH (dose 1.0  $\text{mg}/\text{kg}$ ), administered intravenously (IV) through the tail vein. The fluorescent images were obtained on the Li-COR Pearl<sup>®</sup> Animal Imaging System (LI-COR Biosciences Inc, Lincoln, NE, USA) at 12 hours after IV injection. Mice injected with saline were used as controls.

Approval for the animal studies was obtained from the Oregon State University Institutional Animal Care and Use Committee (IACUC), and the experiments were all conducted in accordance with their policies.

## Results and discussion

### Preparation and characterization

We employed a multistep approach to develop a stable and biocompatible multicomponent nanoplatfor for imaging and PTT-PDT combinatorial therapy. First, LOGr nanosheets, as the PTT agent, were synthesized exploiting aromatic nitronium ion oxidation combined with the unique

properties of microwave heating.<sup>29</sup> These LOGr nanosheets were directly fabricated from graphite without involving any toxic species or metal-containing compounds. As obtained, graphene nanosheets are of uniform size ( $10\pm 4$  nm diameter, with a lateral size around 15 nm and height of 0.8 nm) and have fewer defects, along with great thermal stability. They also exhibit strong wavelength absorption within the visible and NIR regions, without the need for further reduction, owing to the low oxygen content. Notably, the amount of surface functional groups (mostly alcohols and epoxides) is sufficient for further functionalization.<sup>29</sup> Based on X-ray photoelectron spectroscopy (XPS) data, ~56% of the total oxygen functionality is in the form of hydroxyl and epoxy groups.<sup>29</sup> Therefore, freshly prepared LOGr nanosheets were modified with amine-terminated PPIG4 dendrimers, via a nucleophilic ring-opening reaction between the epoxy groups of LOGr and the amine groups of the PPIG4 dendrimer when catalyzed by potassium hydroxide (Figure 1B). The modification with the water-soluble PPIG4 dendrimers improved the stability of the LOGr dispersions in an aqueous environment and introduced the reactive primary amine groups for further functionalization. To introduce a PDT active agent, the PPIG4 dendrimer was initially loaded with Pc, to give the LOGr-Pc-PPIG4 complex with ~20% w/w loading efficiency, as previously described by our group (Figure 1A).<sup>32</sup> To reduce cytotoxicity, LOGr-Pc-PPIG4 complexes were coupled with heterobifunctional 5 kDa PEG polymer (Figure 1C), containing on the opposite ends, an amine-reactive NHS ester and thiol-reactive MAL group. The modification was achieved by the coupling of MAL-PEG-NHS to the amino groups of the dendrimer, at a PPIG4/PEG ratio of 1:16. The introduction of the PEG layer around the dendrimer-graphene nanoplateform resulted in the lower surface charge ( $+6.3\pm 0.9$  mV) as compared with nonmodified complexes ( $+31.6\pm 1.2$  mV). The nearly neutral surface charge will lessen the interaction of the delivery system with macrophages and blood serum proteins during systemic circulation and reduce toxicity linked to cellular membrane damage.<sup>10,30</sup> To improve active intracellular uptake of the PEGylated complex, a cancer-targeting LHRH peptide was conjugated to the LOGr-Pc-PPIG4-PEG (Figure 1C). The receptors for the LHRH peptide are overexpressed on the membranes of both primary and metastatic ovarian cancer cells, including the multidrug-resistant A2780/AD ovarian cancer cells used in this work, but are not evidently expressed in most healthy human tissue.<sup>36-38</sup> Thus, based on this differential expression, the LHRH peptide was chosen for selective targeting to ovarian cancer cells. To attach a

LHRH peptide to the graphene-dendrimer delivery system, the MAL group of the bifunctional PEG-chain was reacted with the thiol group of the cysteine in LHRH (Figure 1C).<sup>10,38</sup> Coupling of the PEGylated complex with LHRH peptide was confirmed by BCA protein assay.<sup>30</sup> In addition, successful LOGr functionalization with Pc-PPIG4, followed by PEG and LHRH peptide modification was confirmed by Fourier transform infrared-attenuated total reflectance (FTIR-ATR) spectroscopy (Figure S1). The average diameter of  $78.3\pm 9.54$  nm, spherical morphology, and the absence of aggregation of the developed LOGr-Pc-PPIG4 nanoplateform were confirmed by AFM (Figure 2A). The detected size of the final nanoplateform is in good agreement with the size combination of the LOGr (~15 nm) and Pc-LHRH (~62 nm).<sup>32</sup> The obtained size is within the range of 10–100 nm, therefore, the developed multifunctional system is expected to have enhanced tumor-targeted delivery via the enhanced permeability and retention (EPR) effect (<200 nm), with the minimal possibility of removal by the kidneys (>10 nm) and detection by macrophage cells (<100 nm).<sup>39,40</sup>

## Photophysical properties of the developed nanoplateform

Water-soluble and sterically stable nanoplateforms with a strong absorption within NIR therapeutic window are required for efficient imaging and combinatorial PDT-PTT therapy.<sup>12,13</sup> Therefore, the stability and spectroscopic properties of the developed PTT-PDT platform (LOGr-Pc-LHRH) were evaluated along with the corresponding controls: PTT (LOGr-LHRH) and PDT (Pc-LHRH) agents. All three studied formulations exhibited excellent solubility in the range of physiological solutions, including PBS buffer and cell culture medium with 10% FBS (Figure 2B), indicating their potential for an efficient *in vivo* application. As shown in Figure 2C, the Pc entrapped in the dendrimer-based nanoplateform exhibited a strong NIR absorption in water, with an absorbance peak at 700 nm (Q-band). The recorded intense NIR absorption fits within the NIR optical biological window essential for fluorescence imaging and an efficient PDT.<sup>41</sup> Unlike Pc, LOGr absorption is not characterized by a well-defined peak at specific wavelengths. However, LOGr absorption displayed relatively uniform strong absorption in the entire NIR region,<sup>29</sup> suggesting that the  $\pi$ -conjugation within the graphene sheets is largely retained. This uniform absorption of the developed LOGr in the NIR range of the spectrum provides a unique possibility for combination with various second-generation photosensitizers to enable activation of the prepared PDT-PTT platforms with a single NIR excitation

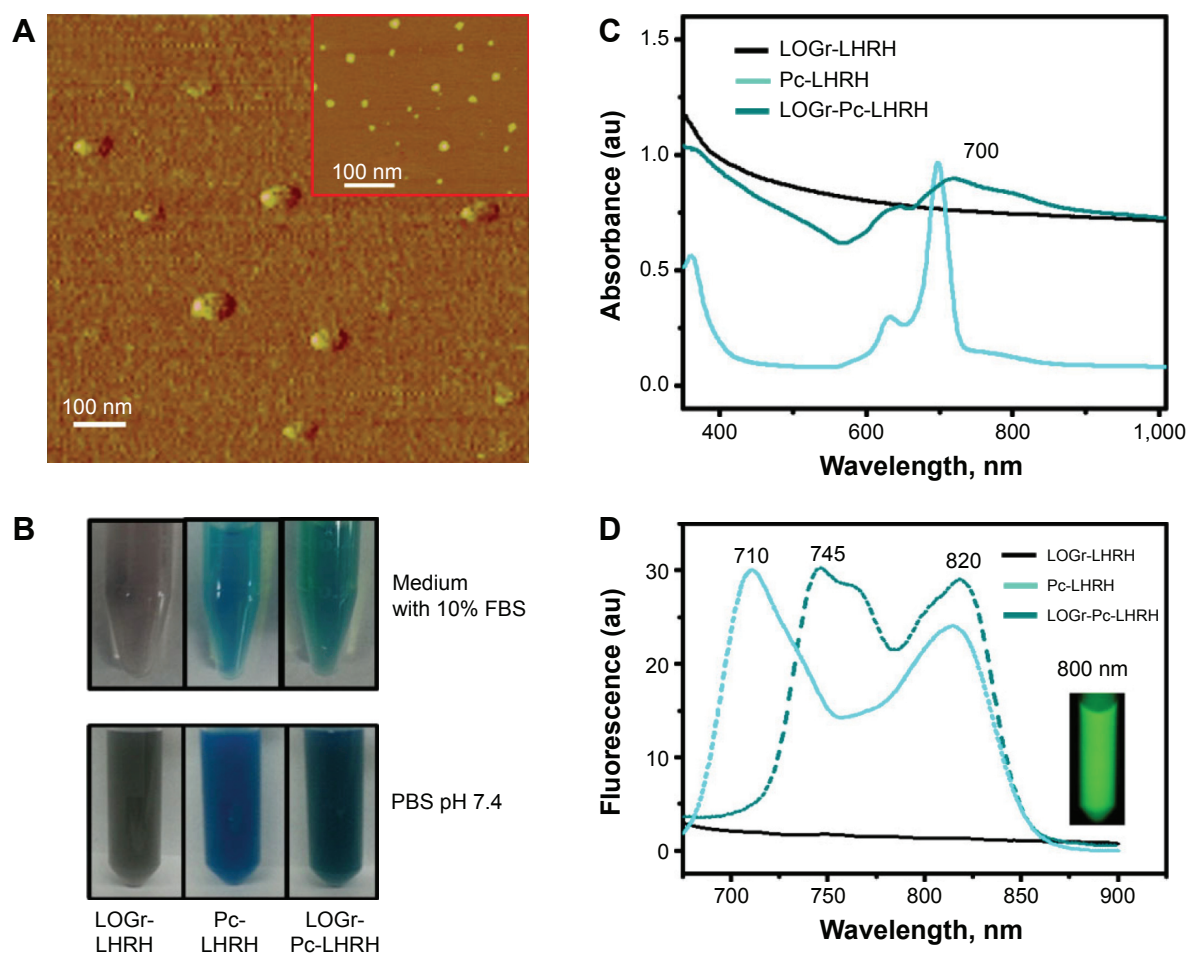


**Figure 2** Characterization of LOGr-Pc-LHRH.

**Notes:** (A) AFM image of LOGr-Pc-LHRH (inset: AFM image of nonmodified LOGr). (B) Stable saturated solutions of LOGr-LHRH, Pc-LHRH, and LOGr-Pc-LHRH, in 1× PBS at pH 7.4 and RPMI 1640 cell culture medium with 10% fetal bovine serum. (C) Absorbance spectra of LOGr-LHRH (black), Pc-LHRH (cyan), and LOGr-Pc-LHRH (dark cyan), in 1× PBS with 10 µg/mL (Pc) and 20 µg/mL LOGr. (D) Fluorescence spectra of LOGr-LHRH (black), Pc-LHRH (cyan), and LOGr-Pc-LHRH (dark cyan), in 1× PBS,  $\lambda_{\text{exc}}=660$  nm with 10 µg/mL (Pc) and 20 µg/mL LOGr (inset: fluorescence images of LOGr-Pc-LHRH in water, recorded with Li-COR Pearl® Animal Imaging System [LI-COR Biosciences Inc, Lincoln, NE, USA] at 800 nm channel).

**Abbreviations:** AFM, atomic force microscopy; FBS, fetal bovine serum; LHRH, luteinizing hormone-releasing hormone; LOGr, low-oxygen graphene; PBS, phosphate-buffered saline; Pc, phthalocyanine; RPMI, Roswell Park Memorial Institute.

wavelength. Notably, modification of LOGr with dendrimer and PEG did not compromise its absorption properties in the NIR spectrum range (Figure 2C). As expected, absorption spectrum of the final LOGr-Pc-LHRH nanoplatform in water revealed the Q-band of Pc (700 nm) superimposed with the absorption curve of LOGr, indicating the presence of both Pc and LOGr within the same delivery system (Figure 2C).

Since photodegradation may greatly affect the efficiency of the photosensitizer, the photostability of Pc encapsulated in the developed nanoplatform was evaluated. According to the obtained results, the photoirradiation of the developed nanoplatform with a 690 nm (0.95 W/cm<sup>2</sup>) diode laser for 10 minutes every 12 hours during 4 days did not demonstrate any decrease in the absorption intensity of Pc (data are not shown), implying photostability of the photosensitizer prior to PDT treatment.

A strong absorption of both PDT and PTT agents at the same wavelengths enables the use of single laser irradiation to concurrently excite both Pc and LOGr to generate ROS, heat, and a fluorescence signal for cancer cell killing and imaging. Our nanoplatform can utilize NIR excitation of a single laser irradiation within the optical transmission window of biological tissues (~650–950 nm), thereby significantly improving penetration depths and minimizing photobleaching background autofluorescence, as well as photodamage to biological specimens.<sup>12,13,42</sup>

Despite a strong absorption signal in the NIR optical window, previously developed nanoplatforms based on hydrophobic interactions and  $\pi$ - $\pi$  stacking between photosensitizers and graphene oxides have been characterized by drastic fluorescence quenching of the photosensitizer and a significant decrease in ROS generation.<sup>24,26,43</sup> This is related to

the fact that graphene contains largely dislocated  $\pi$ -electrons, allowing for energy transfer from the nearby photosensitizers and leading to fluorescence quenching. The indicated properties prevent the application of photosensitizers as the imaging agents and reduce the therapeutic efficacy of PDT.<sup>43</sup> To overcome these obstacles, Pc molecules were encapsulated into hydrophobic pockets of PPIG4 dendrimers to prevent their interactions with LOGr and thus minimize fluorescence quenching.<sup>32</sup> Moreover, the separation of Pc molecules in the dendrimer interior reduces their aggregation, which also leads to the self-quenching effect of the Pc excited state.

In order to evaluate the interaction between LOGr and covalently bound Pc loaded into dendrimer, the fluorescence spectra of LOGr-LHRH, Pc-LHRH, and LOGr-Pc-LHRH in water were assessed. Upon excitation, Pc-LHRH complex in water demonstrated intense fluorescence peaks at 710 nm and 815 nm (Figure 2D). After conjugation with LOGr, the fluorescence spectrum did not indicate a decrease in Pc fluorescence compared with Pc-LHRH alone. This result revealed that the photosensitizer is safely located within the dendrimer, which minimizes its fluorescence quenching, due to the presence of graphene. It is worth mentioning that two fluorescence peaks at 745 nm and 820 nm were slightly shifted compared with those of Pc-LHRH (710 nm and 815 nm). In the final nanoplateform, dendrimer-encapsulated Pc molecules are in close proximity to LOGr, which could cause some electronic interactions between Pc and LOGr, resulting in red-shift in both the absorption and emission spectra. Our data is in good agreement with previous reports, which indicated that interaction between fluorophore and graphene oxide results in red-shifting of the absorption maximum

of the fluorophore.<sup>44,45</sup> Because of the availability of the second emission peak at 820 nm, the fluorescence signal of Pc could be recorded in the far NIR region (Figure 2D, inset), avoiding tissue autofluorescence and light scattering for effective imaging. In contrast, LOGr-LHRH, similar to nonmodified LOGr, does not possess any fluorescence emission within the same NIR region (Figure 2D). The obtained data revealed that protection of Pc within the hydrophobic interior of PPIG4 dendrimers results in sufficient fluorescence emission of the photosensitizer in aqueous solution, indicating no direct interaction between Pc and conjugated LOGr, and thus preserving its imaging and PDT capabilities. Due to the intense absorption and fluorescence within the NIR window, the developed system (LOGr-Pc-LHRH) has a significant potential for application in combinatorial PDT and PTT along with fluorescence imaging.

### Photothermal properties and $^1\text{O}_2$ generation

Due to the strong absorption of LOGr through the wide NIR region, it can be exploited by PTT for deeper cancer tissue treatment, while allowing a PDT agent of appropriate NIR wavelength within this range to facilitate the single-light-induced PDT. Our Pc derivative, excitable at 670–700 nm, is an excellent additive to graphene to achieve the synergetic PTT-PDT effect at a single NIR wavelength. To verify photothermal properties of LOGr and its functionalized derivatives, LOGr, LOGr-LHRH, and LOGr-Pc-LHRH were exposed to the laser at 690 nm, and the temperature change was recorded at 5-minute time intervals for 20 minutes. A temperature increase, of

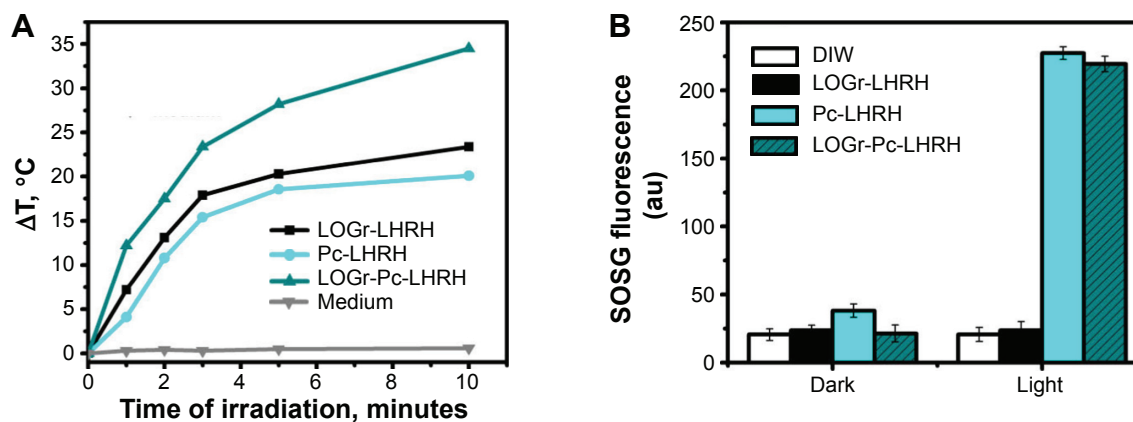


**Figure 3** Heat and singlet oxygen generation by LOGr-Pc-LHRH.

**Notes:** (A) Temperature change upon NIR laser irradiation using 690 nm at 0.95 W/cm<sup>2</sup> for LOGr-LHRH, Pc-LHRH, and LOGr-Pc-LHRH in comparison with cell culture medium as control. (B) Singlet oxygen generation by LOGr-LHRH, Pc-LHRH, and LOGr-Pc-LHRH, after irradiation with 690 nm laser diode (0.3 W/cm<sup>2</sup>) for 5 minutes when compared to DIW and appropriate dark controls. The concentrations of Pc and LOGr in the appropriate formulations were 2  $\mu\text{g}/\text{mL}$  and 3.5  $\mu\text{g}/\text{mL}$ , respectively.

**Abbreviations:** DIW, deionized water; LHRH, luteinizing hormone-releasing hormone; LOGr, low-oxygen graphene; NIR, near-infrared; Pc, phthalocyanine; SOSG, Singlet Oxygen Sensor Green®.

$\Delta T \sim 23^\circ\text{C}$  and  $\sim 20^\circ\text{C}$ , was observed for LOGr-LHRH (LOGr = 20  $\mu\text{g}/\text{mL}$ ) and for Pc-LHRH (Pc = 15  $\mu\text{g}/\text{mL}$ ) in water (Figure 3A), respectively. By converting the absorbed light into heat, Pc-LHRH contributes efficiently to the total amount of heat produced by LOGr-Pc-LHRH. LOGr-Pc-LHRH at the same LOGr and Pc concentration showed a temperature increase of  $\sim 35^\circ\text{C}$ , where the temperature changed rapidly from  $25^\circ\text{C}$  to  $60^\circ\text{C}$  (Figure 3A). These results suggest that 690 nm of the 0.95  $\text{W}/\text{cm}^2$  power light is sufficient to generate mild hyperthermia of the LOGr-containing medium. Moreover, light of this wavelength can be simultaneously used to activate the Pc incorporated in our nanoplatform, for PDT. Pc, as a PDT agent within the LOGr-Pc-LHRH complex, is expected to produce a toxic ROS to kill cancer cells, as  $^1\text{O}_2$  generation is the critical step in PDT. To test the PDT activity of LOGr-Pc-LHRH,  $^1\text{O}_2$  generation by Pc incorporated onto a graphene oxide surface was measured using the SOSG assay, which is exclusively selective toward  $^1\text{O}_2$  and not to other ROS. Samples (LOGr-LHRH, Pc-LHRH, and LOGr-Pc-LHRH) were irradiated with a portable 690 nm laser diode for 5 minutes. As expected, Pc-LHRH showed a  $\sim$  tenfold increase in  $^1\text{O}_2$  production immediately after light exposure. The  $^1\text{O}_2$  generation ability of LOGr-Pc-LHRH was comparable with that of Pc-LHRH (Figure 3B), indicating that the design of our platform does not compromise PDT properties of the Pc within the developed nanoplatform. On the other hand, LOGr-LHRH by itself did not produce a toxic ROS. The obtained data suggest that the combination

of both Pc and LOGr has excellent potential to become a nanoplatform with double therapeutic anticancer properties, ie, as PDT and PTT.

## Cellular uptake and dark cytotoxicity

Sufficient cellular internalization and minimal side effects of both Pc and LOGr under dark conditions (no laser irradiation) are essential for an efficient drug delivery and fluorescence imaging.<sup>46</sup> To evaluate uptake efficiency of the developed nanoplatform for Pc and LOGr into cancer cells, the cellular internalization was assessed by flow cytometry (Figure 4A). The LHRH-positive A2780/AD cancer cells were treated with the LHRH-targeted nanoplatforms for 24 hours, and the flow cytometry data were recorded by detecting the fluorescence signal of the Pc. As seen in Figure 4A, the developed nanoplatforms efficiently transferred the encapsulated Pc through the cellular membrane with comparable efficacy as for both Pc-LHRH and LOGr-Pc-LHRH. The obtained data indicates that the presence of LOGr does not obstruct the cellular internalization properties of the LOGr-Pc-LHRH system. Previously we demonstrated that the cellular internalization efficiency of LHRH-targeted nanocarriers (Pc-LHRH) into LHRH-negative SKOV-3 cancer cells was significantly lower in comparison with LHRH-positive cancer A2780/AD cells.<sup>32</sup>

It has been previously reported that graphene materials without further surface functionalization have limited stability in physiological environments, due to nonspecific binding of proteins to the graphene surface and the screening of

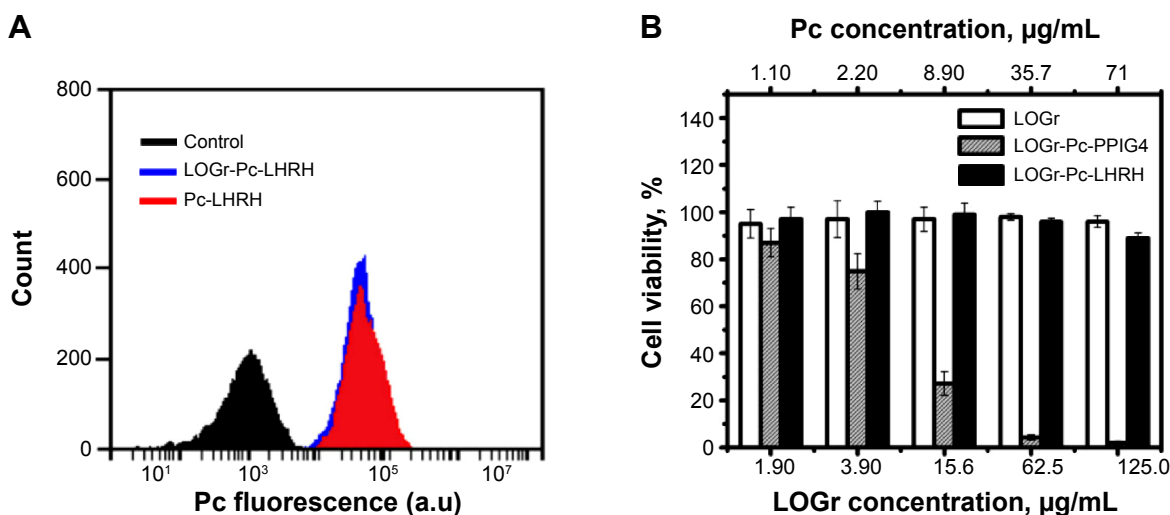


**Figure 4** Cellular uptake and dark cytotoxicity of LOGr-Pc-LHRH.

**Notes:** (A) Flow cytometry analysis of cellular uptake of Pc-LHRH and LOGr-Pc-LHRH nanoplatforms after incubation with the LHRH-positive A2780/AD ovarian cancer cells for 24 hours. (B) Comparative viability of A2780/AD ovarian cancer cells incubated with the different concentrations of unmodified LOGr, LOGr modified with Pc-loaded PPIG4 dendrimer (LOGr-Pc-PPIG4), and LOGr-Pc-PPIG4 modified with PEG and LHRH (LOGr-Pc-LHRH) for 24 hours, under dark conditions.

**Abbreviations:** a.u, arbitrary units; LHRH, luteinizing hormone-releasing hormone; LOGr, low-oxygen graphene; Pc, phthalocyanine; PEG, poly(ethylene glycol); PPIG4, polypropylenimine generation 4.

electrostatic charges.<sup>47,48</sup> Our nonmodified LOGr nanosheets exhibited an enhanced dispersion in water; however, they were not stable in physiological solutions and thus require further functionalization. Similar to other nanomaterials for biomedicine application, the toxicity of graphene is related to its surface functionalization.<sup>10,30</sup> When the A2780/AD cells were treated with increasing concentrations of nonmodified LOGr for 24 hours, no cytotoxicity was recorded when evaluating cell viability using calcein AM assay (Figure 4B). The obtained data suggests that the cancer cells cannot efficiently internalize nonmodified LOGr, as it aggregates in a physiological environment. After modification of LOGr with a Pc-loaded dendrimer, the prepared intermediate LOGr-Pc-PPIG4 complex demonstrated significant dark toxicity toward A2780/AD cells, due to the presence of positively charged amino groups on the dendrimer surface. However, further modification of LOGr-Pc-PPIG4 with biocompatible coatings (PEG and LHRH peptide) resulted in the final nanoplateform (LOGr-Pc-LHRH), which did not express cytotoxic behavior at the highest tested concentration of 71.0  $\mu\text{g/mL}$  for Pc (125  $\mu\text{g/mL}$  of LOGr) (Figure 4B). At the same time, the cancer cells efficiently internalized the prepared nanoplateform, as was shown with flow cytometry data (Figure 4A). Moreover, it exhibited excellent stability in the cell culture medium supplemented with FBS (Figure 2B).

Prevention of drug release in the systemic circulation and, thus, minimal blood toxicity is desired for an effective delivery system. PDT-PTT platforms based on  $\pi$ - $\pi$  stacking interaction between photosensitizers and graphene can result in leakage of PDT agents during their circulation in

the blood stream. In our approach, the encapsulation of Pc in the interior PPIG4 dendrimer limits the release of photosensitizer in the biological media, and thus decreases its toxicity during systemic circulation and ensures simultaneous delivery of both PDT and PTT agents to the cancer cells. To investigate cytotoxicity toward red blood cells (RBCs), hemolysis studies were carried out on the developed nanoplateforms (LOGr-LHRH, Pc-LHRH, and LOGr-Pc-LHRH) at various concentrations. As shown in Figure 5A, the prepared formulations showed minimal hemolytic activity, even at the highest studied LOGr concentration (44  $\mu\text{g/mL}$ ), indicating minimal blood toxicity. The obtained data suggests that the graphene surface does not appear to be toxic toward RBCs after modification with PEG and LHRH. Pc itself should not cause any toxicity, as it stays within the dendrimer in aqueous media.<sup>32</sup> To prove this point, the Pc release profile of the developed formulation was evaluated in PBS buffer at pH 7.4, in 50% human plasma, and in the presence of 10 mM of reduced glutathione (PBS, pH 5.5), simulating intracellular conditions (Figure 5B). The results demonstrated the minimal (less than 2%) drug release. Thus, it can be anticipated that the encapsulated photosensitizers, due to their very hydrophobic nature, are not able to escape from the dendrimer-based carrier in an intracellular environment, and hence, they cannot directly induce toxicity.

## Combinatorial PDT-PTT treatment

To evaluate the efficiency of the new nanoplateform as a PTT-PDT agent, the phototherapeutic effect of the LOGr-Pc-LHRH complex on ovarian cancer cells was evaluated.

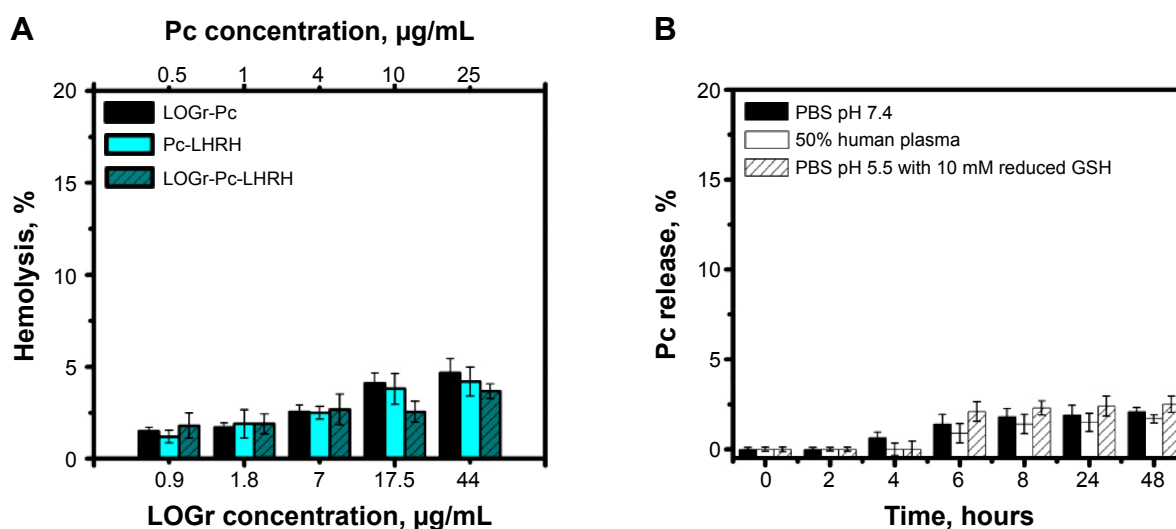


**Figure 5** Hemolytic activity and drug release by LOGr-Pc-LHRH.

**Notes:** (A) Hemolysis of red blood cells after incubation with LOGr-LHRH, Pc-LHRH, and LOGr-Pc-LHRH at various concentrations. (B) The release profiles of Pc from LOGr-Pc-LHRH complex incubated at 37°C, in PBS buffer at pH 7.4, in PBS buffer at pH 5.5 with 10mM reduced GSH, and in 50% human plasma.

**Abbreviations:** GSH, glutathione; LHRH, luteinizing hormone-releasing hormone; LOGr, low-oxygen graphene; PBS, phosphate-buffered saline; Pc, phthalocyanine.

A2780/AD ovarian cancer cells were treated with the developed LOGr-Pc-LHRH complex at low Pc (1.0–4.0  $\mu\text{g/mL}$ ) and LOGr (1.8–7.0  $\mu\text{g/mL}$ ) concentrations for 18 hours and then irradiated by a laser diode of relatively low power (0.3  $\text{W/cm}^2$ ) at 690 nm for 15 minutes, followed by viability measurements in 24 hours. Under dark, toxicity of the LOGr-Pc-LHRH complex was insignificant (Figure 4B), whereas pronounced cytotoxicity was detected upon the NIR irradiation (Figure 6A). When the two treatments (PTT and PDT) were combined under a single 690 nm light irradiation, the A2780/AD ovarian cancer cell viability was remarkably reduced with the LOGr-Pc-LHRH as compared with LOGr-LHRH (PTT) and Pc-LHRH (PDT) alone, at the

same concentrations. We also observed that the synergetic phototherapeutic effect (PTT and PDT) of the LOGr-Pc-LHRH was most pronounced at low concentrations of Pc ( $<4.0 \mu\text{g/mL}$ ). At higher Pc concentrations in the LOGr-Pc-LHRH system, the PDT began to dominate over PTT. Thus, cancer cell treatment with the LOGr-Pc-LHRH (Pc of  $\sim 2 \mu\text{g/mL}$  and LOGr  $\sim 3.5 \mu\text{g/mL}$ ) following 15 minutes of light irradiation resulted in only 5% of the cells surviving, while the cell viability after treatment with LOGr-LHRH and Pc-LHRH at the same LOGr and Pc concentrations was 75% and 27%, respectively (Figure 6A). Thus, at low concentrations, the LOGr-Pc-LHRH exhibits pronounced synergetic effect by utilizing properties of both PDT and PTT.

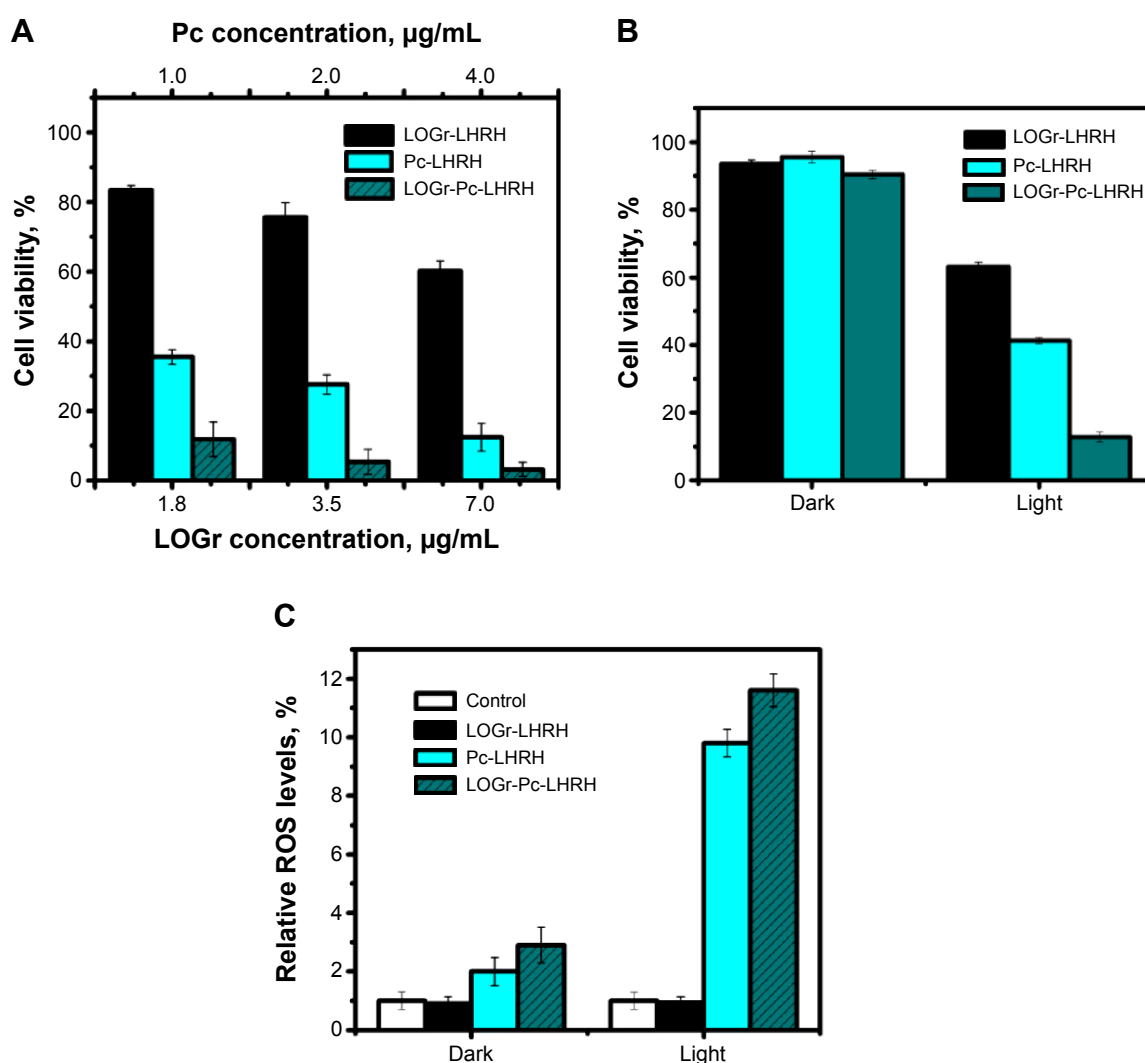


**Figure 6** Combinatorial PDT-PTT treatment.

**Notes:** (A) Combinatorial (PDT-PTT) therapeutic effects of LOGr-Pc-LHRH on A2780/AD cells (10,000) incubated with different Pc (LOGr) concentrations and irradiated for 15 minutes using a 690 nm laser diode (0.3  $\text{W/cm}^2$ ), compared with controls. (B) Combinatorial (PDT-PTT) therapeutic effects of LOGr-Pc-LHRH on A2780/AD cell pellets (2,000,000) irradiated for 10 minutes using a 690 nm laser diode (0.95  $\text{W/cm}^2$ ), compared with controls. (C) Relative intracellular ROS levels in A2780/AD cells incubated with LOGr-Pc-LHRH at Pc concentration of 2  $\mu\text{g/mL}$  (LOGr = 3.5  $\mu\text{g/mL}$ ) and irradiated for 5 minutes using a 690 nm laser diode (0.3  $\text{W/cm}^2$ ), compared with controls. Untreated cells and cells treated with nanoplatfrom under dark conditions were used as controls.

**Abbreviations:** LHRH, luteinizing hormone-releasing hormone; LOGr, low-oxygen graphene; Pc, phthalocyanine; PDT, photodynamic therapy; PTT, photothermal therapy; ROS, reactive oxygen species.

Thus, a synergistic effect of the combinatorial treatment was achieved with the developed nanoplateform and was greater compared with each of the two treatments applied separately, as evaluated according to Valeriote's formula. Based on the data, the Pc molecules do not need to be released from the LOGr-Pc-LHRH system to cause the PDT effect in cancer cells. The observed results support previous observations by Kojima et al<sup>49</sup> and by our team,<sup>32</sup> which suggest that diffusion of the generated ROS around the delivery system in the cell might be sufficient for therapeutic effects.

In addition, to mimic an ovarian cancer tumor, A2780/AD pellets, containing ~2,000,000 cells, were treated with LOGr-Pc-LHRH, followed by irradiation with the laser diode of slightly higher but still in the low-range power (0.95 W/cm<sup>2</sup>) at 690 nm for 10 minutes. The results confirmed the synergistic effect of the developed PTT-PDT nanoplateform, with only ~10% cell survival compared with LOGr-LHRH (60%) and Pc-LHRH (40%) using the same phototherapy conditions (Figure 6B). The laser power of 0.95 W/cm<sup>2</sup> appears to be safe without obvious A2780/AD cell death after 690 nm laser irradiation for 10–15 minutes.

The above data evidently suggest that our system can only be activated for combined therapy by NIR light; otherwise, the graphene-based nanoplateform is not cytotoxic under dark conditions (in the absence of external NIR light). This demonstrates that we can achieve synergistic therapeutic effects for ovarian cancer treatment with the developed LOGr-Pc-LHRH nanoplateform using single wavelength laser irradiation. The cell death in the presence of LOGr-Pc-LHRH after exposure to 690 nm light can be triggered by the combination of mechanisms – ROS production and mild hyperthermia. The current data is in good agreement with our previous work, in which mild hyperthermia was used for cancer treatment, maintaining the temperature of the A2780/AD cancer cells at 40°C. It was indicated that intracellular mild hyperthermia delivered significantly reduced viability of drug-resistant ovarian cancer cells.<sup>10</sup>

### Intracellular ROS generation

The intracellular generation of cytotoxic ROS by the photosensitizer upon light activation would confirm a key mechanism of PDT-induced cell death.<sup>7,50</sup> Hence, the influence of PDT mediated by LOGr-Pc-LHRH complexes, on the ROS level within A2780/AD cells was assessed by DCFH-DA assay and compared with different controls: (a) untreated cells, (b) cells treated with light only, (c) cells treated with LOGr-LHRH, (d) cells treated with Pc-LHRH, and (e) cells treated with LOGr-Pc-LHRH without laser treatment.

The control samples showed similar ROS levels, proposing that the recorded increase in ROS generation is the result of the PDT effect of the developed nanoplateform after activation by NIR light. As seen in Figure 6C, cells exposed to LOGr-Pc-LHRH (Pc of ~2 µg/mL and LOGr ~3.5 µg/mL) and then subsequently irradiated with the 690 nm diode laser light for 5 minutes showed a pronounced elevation in intracellular ROS level in comparison with those treated with the same formulation but without laser exposure. Treatment of cancer cells with Pc (3.5 µg/mL) in LOGr-Pc-LHRH followed by a 5-minute light exposure increased the general ROS levels by 11.6-fold compared with the controls and was comparable with that of Pc-LHRH alone. LOGr-LHRH did not produce toxic ROS under applied light irradiation. Thus, the elevated intracellular ROS level after PDT treatment may be the one of main reasons for the enhanced phototoxicity with LOGr-Pc-LHRH.

### In vivo NIR imaging

To confirm the ability of the designed system to target cancer tumors and to perform as an NIR imaging agent in vivo, LOGr-Pc-LHRH complexes were administered into mice bearing ovarian cancer tumor via tail vein IV injection. The NIR fluorescence images were obtained with a Li-COR Pearl Animal Imaging System at 800 nm. Figure 7 shows the in vivo whole-body images of mice injected with

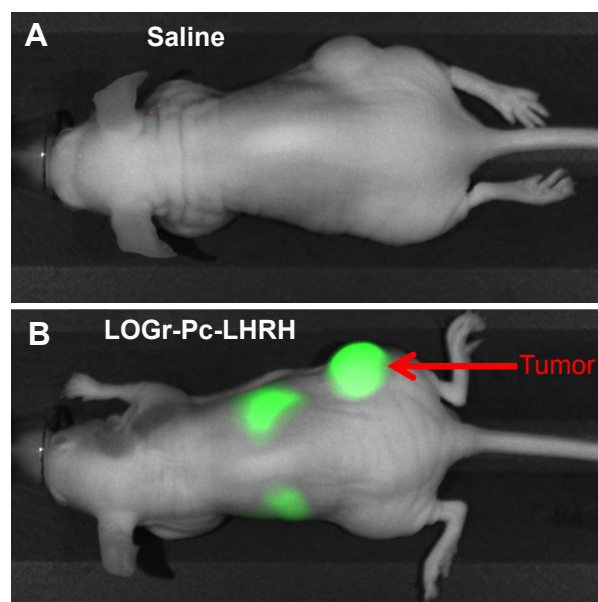


**Figure 7** In vivo NIR fluorescence imaging of nude mice bearing A2780/AD tumor after IV injection of saline (**A**) and LOGr-Pc-LHRH (**B**) at 12 hours postinjection, using the Li-COR Pearl<sup>®</sup> Animal Imaging System (LI-COR Biosciences Inc, Lincoln, NE, USA).

**Abbreviations:** IV, intravenous; LHRH, luteinizing hormone-releasing hormone; LOGr, low-oxygen graphene; NIR, near-infrared; Pc, phthalocyanine.

LOGr-Pc-LHRH and saline as control. The strong fluorescence signal detected, at 12 hours postinjection, in various tissues of mice, including the cancer tumor, suggests that Pc loaded into a graphene-dendrimer nanoplatfom can be used as a fluorescence agent for NIR imaging-guided drug delivery (Figure 7). A significant fluorescence signal was observed in the tumor area, suggesting the tumor-targeting ability of the delivery system. No fluorescence signal was detected in mice before LOGr-Pc-LHRH injection or after the injection with saline, indicating that the recorded fluorescence signal as not related to tissue autofluorescence. Our data is in good agreement with the previously reported in vivo imaging results for Pc-LHRH alone.<sup>32</sup>

## Conclusion

Herein we report a convenient approach for building a novel theranostic platform (LOGr-Pc-LHRH) to deliver PDT drug (Pc) and PTT agent (graphene nanosheets) for combinatorial ovarian cancer therapy and imaging. Our new platform demonstrated good biocompatibility, strong NIR optical properties, and excellent physiological stability, along with photostability and drug delivery efficiency essential for an effective phototherapeutic system. In the absence of NIR light, no cytotoxicity has been observed for LOGr-Pc-LHRH. Upon irradiation, the LOGr-Pc-LHRH rapidly converts optical energy into heat and generates ROS to kill cancer. Compared with PDT and PTT alone, combinatorial PTT-PDT cancer treatment shows synergistic therapeutic effects under external NIR light activation. Conveniently, a low-power irradiation of single wavelength (690 nm) within the NIR optical window can be used for both the ROS production by Pc and heat generation by LOGr. In addition, the unique molecular design prevents fluorescence quenching of Pc by graphene nanosheets, allowing for fluorescence imaging. The new nanoplatfom functions as an effective delivery and protective system for LOGr (PTT) and Pc (PDT), exhibiting pronounced theranostic properties for application in imaging and phototherapy treatment of unresected ovarian cancer tumors.

## Acknowledgments

This work was supported by the Pharmaceutical Research and Manufacturers of America Foundation, the Medical Research Foundation of Oregon, the College of Pharmacy at Oregon State University, and the National Science Foundation (grant number CBET 1438493). We are thankful to Dr B Dolan and A Palmer of the College of Veterinary Medicine, Oregon State University, for their help with the flow cytometry analysis.

## Disclosure

The authors report no conflicts of interest in this work.

## References

- Al Rawahi T, Lopes AD, Bristow RE, et al. Surgical cytoreduction for recurrent epithelial ovarian cancer. *Cochrane Database Syst Rev*. 2013;2:CD008765.
- Robinson WR, Beyer J, Griffin S, Kanjanavaikoon P. Extraperitoneal metastases from recurrent ovarian cancer. *Int J Gynecol Cancer*. 2012;22(1):43–46.
- Bristow RE, Karlan BY, Chi DS. *Surgery for Ovarian Cancer: Principles and Practice*. 2nd ed. New York, NY: Informa Healthcare; 2010.
- Gottesman MM. Mechanisms of cancer drug resistance. *Ann Rev Med*. 2002;53:615–627.
- Oh J, Yoon H, Park JH. Nanoparticle platforms for combined photothermal and photodynamic therapy. *Biomed Eng Lett*. 2013;3:67–73.
- Taratula O, Schumann C, Duong T, Taylor KL, Taratula O. Dendrimer-encapsulated naphthalocyanine as a single agent-based theranostic nanoplatfom for near-infrared fluorescence imaging and combinatorial anticancer phototherapy. *Nanoscale*. 2015;7(9):3888–3902.
- Dolmans DE, Fukumura D, Jain RK. Photodynamic therapy for cancer. *Nat Rev Cancer*. 2003;3(5):380–387.
- Huang HW, Liah CT. Review: Therapeutical applications of heat in cancer therapy. *J Med Biol Eng*. 2012;32(1):1–10.
- Levi-Polyachenko NH, Stewart JH IV. Clinical relevance of nanoparticle induced hyperthermia for drug delivery and treatment of abdominal cancers. *Open Nanomed J*. 2011;3:24–37.
- Taratula O, Dani RK, Schumann C, et al. Multifunctional nanomedicine platform for concurrent delivery of chemotherapeutic drugs and mild hyperthermia to ovarian cancer cells. *Int J Pharm*. 2013;458(1):169–180.
- Yanase S, Nomura J, Matsumura Y, Kato H, Tagawa T. Hyperthermia enhances the antitumor effect of photodynamic therapy with ALA hexyl ester in a squamous cell carcinoma tumor model. *Photodiagnosis Photodyn Ther*. 2012;9(4):369–375.
- Josefsen LB, Boyle RW. Unique diagnostic and therapeutic roles of porphyrins and phthalocyanines in photodynamic therapy, imaging and theranostics. *Theranostics*. 2012;2(9):916–966.
- Sekkat N, van den Bergh H, Nyokong T, Lange N. Like a bolt from the blue: phthalocyanines in biomedical optics. *Molecules*. 2012;17(1):98–144.
- Josefsen LB, Boyle RW. Photodynamic therapy and the development of metal-based photosensitizers. *Met Based Drugs*. 2008;2008:276109.
- von Maltzahn G, Park JH, Agrawal A, et al. Computationally guided photothermal tumor therapy using long-circulating gold nanorod antennas. *Cancer Res*. 2009;69(9):3892–3900.
- Liu H, Chen D, Li L, et al. Multifunctional gold nanoshells on silica nanorattles: a platform for the combination of photothermal therapy and chemotherapy with low systemic toxicity. *Angew Chem Int Ed Engl*. 2011;50(4):891–895.
- Liu J, Cui L, Losic D. Graphene and graphene oxide as new nanocarriers for drug delivery applications. *Acta Biomater*. 2013;9(12):9243–9257.
- Kim H, Lee D, Kim J, Kim TI, Kim WJ. Photothermally triggered cytosolic drug delivery via endosome disruption using a functionalized reduced graphene oxide. *ACS Nano*. 2013;7(8):6735–6746.
- Robinson JT, Tabakman SM, Liang Y, et al. Ultrasmall reduced graphene oxide with high near-infrared absorbance for photothermal therapy. *J Am Chem Soc*. 2011;133(17):6825–6831.
- Yang K, Wan J, Zhang S, Tian B, Zhang Y, Liu Z. The influence of surface chemistry and size of nanoscale graphene oxide on photothermal therapy of cancer using ultra-low laser power. *Biomaterials*. 2012;33(7):2206–2214.

21. Wang Y, Wang H, Liu D, Song S, Wang X, Zhang H. Graphene oxide covalently grafted upconversion nanoparticles for combined NIR mediated imaging and photothermal/photodynamic cancer therapy. *Biomaterials*. 2013;34(31):7715–7724.
22. Sahu A, Choi WI, Lee JH, Tae G. Graphene oxide mediated delivery of methylene blue for combined photodynamic and photothermal therapy. *Biomaterials*. 2013;34(26):6239–6248.
23. Guo M, Mao H, Li Y, et al. Dual imaging-guided photothermal/photodynamic therapy using micelles. *Biomaterials*. 2014;35(16):4656–4666.
24. Tian B, Wang C, Zhang S, Feng L, Liu Z. Photothermally enhanced photodynamic therapy delivered by nano-graphene oxide. *ACS Nano*. 2011;5(9):7000–7009.
25. Jiang BP, Hu LF, Wang DJ, Ji SC, Shen XC, Liang H. Graphene loading water-soluble phthalocyanine for dual-modality photothermal/photodynamic therapy via a one-step method. *J Mater Chem B*. 2014; 2:7141–7148.
26. Gollavelli G, Ling YC. Magnetic and fluorescent graphene for dual modal imaging and single light induced photothermal and photodynamic therapy of cancer cells. *Biomaterials*. 2014;35(15):4499–4507.
27. Rong P, Yang K, Srivastan A, et al. Photosensitizer loaded nano-graphene for multimodality imaging guided tumor photodynamic therapy. *Theranostics*. 2014;4(3):229–239.
28. Zhu J, Li Y, Chen Y, et al. Graphene oxide covalently functionalized with zinc phthalocyanine for broadband optical limiting. *Carbon*. 2011; 49(6):1900–1905.
29. Patel MA, Yang H, Chiu PL, et al. Direct production of graphene nanosheets for near infrared photoacoustic imaging. *ACS Nano*. 2013; 7(9):8147–8157.
30. Taratula O, Garbuzenko OB, Kirkpatrick P, et al. Surface-engineered targeted PPI dendrimer for efficient intracellular and intratumoral siRNA delivery. *J Control Release*. 2009;140(3):284–293.
31. Miao W, Shim G, Lee S, Lee S, Choe YS, Oh YK. Safety and tumor tissue accumulation of pegylated graphene oxide nanosheets for co-delivery of anticancer drug and photosensitizer. *Biomaterials*. 2013;34(13):3402–3410.
32. Taratula O, Schumann C, Naleway MA, Pang AJ, Chon KJ, Taratula O. A multifunctional theranostic platform based on phthalocyanine-loaded dendrimer for image-guided drug delivery and photodynamic therapy. *Mol Pharm*. 2013;10(10):3946–3958.
33. Savla R, Taratula O, Garbuzenko O, Minko T. Tumor targeted quantum dot-mucin I aptamer-doxorubicin conjugate for imaging and treatment of cancer. *J Control Release*. 2011;153(1):16–22.
34. Yildirim A, Ozgur E, Bayindir M. Impact of mesoporous silica nanoparticle surface functionality on hemolytic activity, thrombogenicity and non-specific protein adsorption. *J Mater Chem B*. 2013; 1:1909–1920.
35. Kimani SG, Shmigol TA, Hammond S, et al. Fully protected glycosylated zinc (II) phthalocyanine shows high uptake and photodynamic cytotoxicity in MCF-7 cancer cells. *Photochem Photobiol*. 2013;89(1):139–149.
36. Dharap SS, Wang Y, Chandna P, et al. Tumor-specific targeting of an anticancer drug delivery system by LHRH peptide. *Proc Natl Acad Sci U S A*. 2005;102(36):12962–12967.
37. Nagy A, Schally AV. Targeting of cytotoxic luteinizing hormone-releasing hormone analogs to breast, ovarian, endometrial, and prostate cancers. *Biol Reprod*. 2005;73(5):851–859.
38. Shah V, Taratula O, Garbuzenko OB, Taratula OR, Rodriguez-Rodriguez L, Minko T. Targeted nanomedicine for suppression of CD44 and simultaneous cell death induction in ovarian cancer: an optimal delivery of siRNA and anticancer drug. *Clin Cancer Res*. 2013;19(22):6193–6204.
39. Alexis F, Pridden E, Molnar LK, Farokhzad OC. Factors affecting the clearance and biodistribution of polymeric nanoparticles. *Mol Pharm*. 2008;5(4):505–515.
40. Maruyama K. Intracellular targeting delivery of liposomal drugs to solid tumors based on EPR effects. *Adv Drug Deliv Rev*. 2011;63(3): 161–169.
41. MacDonald IJ, Dougherty TJ. Basic principles of photodynamic therapy. *J Porphyrins Phthalocyanines*. 2001;05(2):105–129.
42. Pansare V, Hejazi S, Faenza W, Prud'homme RK. Review of long-wavelength optical and NIR imaging materials: contrast agents, fluorophores and multifunctional nano carriers. *Chem Mater*. 2012; 24(5):812–827.
43. Huang P, Xu C, Lin J, et al. Folic acid-conjugated graphene oxide loaded with photosensitizers for targeting photodynamic therapy. *Theranostics*. 2011;1:240–250.
44. Bozkurt E, Acar M, Onganer Y, Meral K. Rhodamine 101-graphene oxide composites in aqueous solution: the fluorescence quenching process of rhodamine 101. *Phys Chem Chem Phys*. 2014;16(34):18276–18281.
45. Geng J, Jung HT. Porphyrin functionalized graphene sheets in aqueous suspensions: from the preparation of graphene sheets to highly conductive graphene films. *J Phys Chem C*. 2010;114(18):8227–8234.
46. Almeida RD, Manadas BJ, Carvalho AP, Duarte CB. Intracellular signaling mechanisms in photodynamic therapy. *Biochim Biophys Acta*. 2004;1704(2):59–86.
47. Kim MG, Park JY, Shon Y, Shim G, Oh YK. Pharmaceutical applications of graphene-based nanosheets. *Curr Pharm Biotechnol*. 2014;14(12):1016–1026.
48. Yang K, Zhang S, Zhang G, Sun X, Lee ST, Liu Z. Graphene in mice: ultrahigh in vivo tumor uptake and efficient photothermal therapy. *Nano Lett*. 2010;10(9):3318–3323.
49. Kojima C, Toi Y, Harada A, Kono K. Preparation of poly(ethylene glycol)-attached dendrimers encapsulating photosensitizers for application to photodynamic therapy. *Bioconjugate Chem*. 2007;18(3):663–670.
50. Agostinis P, Berg K, Cengel KA, et al. Photodynamic therapy of cancer: an update. *CA Cancer J Clin*. 2011;61(4):250–281.

## Supplementary materials

### Fourier transform infrared-attenuated total reflectance (FTIR-ATR) studies

FTIR-ATR measurements of the freeze-dried samples were conducted using a Nicolet iS5 FTIR Spectrometer equipped with iD7-ATR (Thermo Fisher Scientific, Waltham, MA, USA). The FTIR-ATR spectra were acquired within the 4,000–400  $\text{cm}^{-1}$  spectral region. Background spectra of a clean attenuated total reflectance (ATR) surface were acquired prior to each sample measurement, using the same acquisition parameters.

FTIR-ATR spectroscopic measurements were performed to confirm the presence of poly(ethylene glycol) (PEG) and luteinizing hormone-releasing hormone (LHRH) after functionalization of low-oxygen graphene (LOGr). Figure S1 shows the comparison of the FTIR-ATR spectral features of nonmodified LOGr and LOGr functionalized first with polypropylenimine generation 4 (PPIG4) dendrimer

loaded with phthalocyanine (Pc) derivative (Pc-PPIG4), and finally with PEG and LHRH peptide. As expected, nonmodified LOGr showed barely noticeable peaks at  $\sim 3,400$ , 2,100, 1,580, and 1,250  $\text{cm}^{-1}$  (Figure S1), possibly corresponding to C-C stretch and oxygen-related groups, such as hydroxyl and epoxy groups. When modified with Pc-PPIG4, the ATR spectrum showed distinguished peaks related to the PPIG4 dendrimer structure (Figure S1A and B) as well as to Pc structure. After further functionalization with PEG and LHRH peptide, Figure S1A revealed the spectrum where the corresponding numbers of peaks identifying to PEG and LHRH structures were observed (Figure S1B). In particular, characteristic bands of PEG at  $\sim 2,880$  (C-H) and  $\sim 1,100$  (C-O-C)  $\text{cm}^{-1}$  were clearly observed in the ATR spectrum of the final (LOGr-Pc-LHRH) freeze-dried sample (Figure S1A). In addition, presence of LHRH peptide was also confirmed via quite strong bands at  $\sim 3,270$  (O-H, N-H) and  $\sim 1,650$  (C=O)  $\text{cm}^{-1}$ .

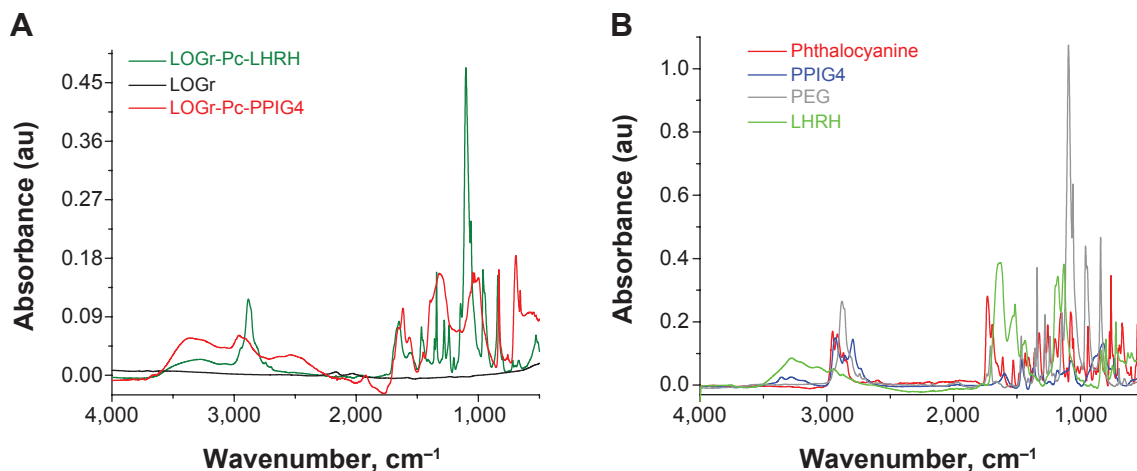


**Figure S1** FTIR-ATR characterization of LOGr-Pc-LHRH.

**Notes:** (A) FTIR-ATR spectra of nonmodified LOGr (black line), LOGr-Pc-PPIG4 (red line), and LOGr-Pc-LHRH (green line). (B) FTIR-ATR spectra of controls: Pc (red line), PPIG4 (blue line), PEG (gray line), and LHRH (green line).

**Abbreviations:** FTIR-ATR, Fourier transform infrared-attenuated total reflectance; LHRH, luteinizing hormone-releasing hormone; LOGr, low-oxygen graphene; Pc, phthalocyanine; PEG, poly(ethylene glycol); PPIG4, polypropylenimine generation 4.

International Journal of Nanomedicine

Publish your work in this journal

The International Journal of Nanomedicine is an international, peer-reviewed journal focusing on the application of nanotechnology in diagnostics, therapeutics, and drug delivery systems throughout the biomedical field. This journal is indexed on PubMed Central, MedLine, CAS, SciSearch®, Current Contents®/Clinical Medicine,

Submit your manuscript here: <http://www.dovepress.com/international-journal-of-nanomedicine-journal>

Dovepress

Journal Citation Reports/Science Edition, EMBase, Scopus and the Elsevier Bibliographic databases. The manuscript management system is completely online and includes a very quick and fair peer-review system, which is all easy to use. Visit <http://www.dovepress.com/testimonials.php> to read real quotes from published authors.